

New Molecular Architecture for Electrically Conducting Materials Based on Unsymmetrical Organometallic-Dithiolene Complexes

Kazuya Kubo and Reizo Kato

Abstract New molecular architecture for highly conducting molecular materials was developed with use of unsymmetrical organometallic-dithiolene complexes. The new architecture has various advantages including easy modification of their molecular and electronic features. Organometallic complexes based on unsymmetrical Au(III)-dithiolene complexes [(ppy)Au(C₈H₄S₈ or C₈H₄S₆O₂)] were prepared for new cationic components of molecular conductors. These unsymmetrical organometallic complexes can provide various cation radical salts [(ppy)Au(S-S)]₂[anion][solvent]_n (S-S = C₈H₄S₈ or C₈H₄S₆O₂, anion = PF₆[−], BF₄[−], AsF₆[−], TaF₆[−], solvent = PhCl, n = 0–0.5) by constant current electrolysis of their benzonitrile or chlorobenzene solutions containing (Bu₄N)(anion) as electrolyte. [(ppy)Au(C₈H₄S₈)]₂[PF₆] under pressure is the first molecular metal based on the organometallic component. In this review, principle of the molecular architecture based on the unsymmetrical organometallic-dithiolene complexes and physical properties of their cation radical salts are discussed.

Keywords Donor type metal complexes, Metal dithiolene complexes, Molecular conductors, Organometallic complexes, Unsymmetrical metal complexes

Contents

1	General Introduction of Molecular Conductors	37
1.1	General Features of Molecular Conductors	37
1.2	Molecular Conductors Based on Metal Complexes	39
1.3	Molecular Conductors Based on Cationic Metal Complexes	40
2	Unsymmetrical Components Based on Diimine–Dithiolene Complexes	40
2.1	Molecular Design of Unsymmetrical Components Based on Diimine–Dithiolene Complexes	40

K. Kubo(✉) and R. Kato

Condensed Molecular Materials Laboratory, 2-1 Hirosawa, Wako-shi, Saitama, 351-0198, Japan,
E-mail: kkubo@riken.jp

2.2	Cation Radical Salts of the Unsymmetrical Diimine–Dithiolene Complexes	41
2.3	Conclusion	42
3	Unsymmetrical Components Based on Organometallic–Dithiolene Complexes	43
3.1	General Features of Unsymmetrical Components Based on Organometallic Metal–Dithiolene Complexes	43
3.2	Cation Radical Salts of the Organometallic Au(III) Dithiolene Complexes	44
3.3	Conclusion	48
4	Other Unsymmetrical Organometallic–Dithiolene Complexes for the Components of Molecular Conductors	50
5	General Conclusion	50
	References	52

Abbreviations

BEDT-TTF	Bis(ethylenedithio)tetrathiafulvalene
bpy	2,2'-Bipyridine
Bu-pia	<i>N</i> -Butyl-pyridine-carbaldimine
CH ₂ Cl ₂	Dichloromethane
C ₈ H ₄ S ₈ ²⁻	2-[(4,5-Ethylenedithio)-1,3-dithiole-2-ylidene]-1,3-dithiole-4,5-dithiolate(2-)
C ₈ H ₄ S ₆ O ₂ ²⁻	2-[(4,5-Ethylenedioxio)-1,3-dithiole-2-ylidene]-1,3-dithiole-4,5-dithiolate(2-)
CT	Charge transfer
DCNQI	<i>N,N'</i> -Dicyanoquinonediimine
dddt	5,6-Dihydro-1,4-dithiin-2,3-dithiolate
Dec-pia	<i>N</i> -Decyl-pyridine-carbaldimine
dmit ²⁻	1,3-Dithiole-2-thiol-4,5-dithiolate(2-)
Et-pia	<i>N</i> -Ethyl-pyridine-carbaldimine
Hexdec-pia	<i>N</i> -Hexadecyl-pyridine-carbaldimine
HOMO	Highest occupied molecular orbital
IR	Infrared
LUMO	Lowest unoccupied molecular orbital
mnt	Maleonitriledithiolate
MO	Molecular orbital
PhCl	Chlorobenzene
phen	1,10-Phenanthroline
ppy ⁻	<i>C</i> -Dehydro-2-phenylpyridine
Pr ⁱ -pia	<i>N</i> -Iso-propyl-pyridine-carbaldimine
TCNQ	7,7,8,8-Tetracyano- <i>p</i> -quinodimethane
tmdt	Trimethylenetetrathiafulvalenedithiolate
TTF	Tetrathiafulvalene

1 General Introduction of Molecular Conductors

1.1 General Features of Molecular Conductors

Since the discovery of the first organic semiconductor perylene-bromine complex in 1954 [1], a large number of molecular conductors, including more than 100 molecular superconductors, have been prepared. Conducting molecular materials are characterized by the following features;

1. Clear and simple electronic structure which can be well described by the tight-binding band picture based on the extended Hückel molecular orbital calculation [2]
2. A variety of physical properties that originate from low-dimensionality, strongly correlated electron-electron interaction, frustration effect, and so on
3. Softness of the crystal lattice and sensitivity to external stimuli
4. Plenty of possibilities for chemical design

Thanks to these characteristics, the molecular conductor is now one of the standard materials in condensed matter physics and interdisciplinary basic science is expanding.

In general, component molecules for molecular conductors (Fig. 1) belong to the π -conjugated system and are divided into two categories, electron donor and electron acceptor. The component molecule is an insulator in itself. In order to obtain the metallic state, the formation of at least one partially filled energy band is required. A straightforward access to the molecular metal can be achieved by arranging open-shell molecules (radicals) so as to enable intermolecular electron transfer. In most cases, cation radicals or anion radicals generated from the donor or the acceptor have been used for the formation of metallic molecular crystals, and the conduction band originate from HOMO of the donor or LUMO of the acceptor. It should be added that electron transfer between HOMO and LUMO bands in a single-component molecular crystal can also generate partially filled energy bands, which is observed in the first single-component molecular metal Ni(tmdt)₂ (Fig. 1) where an energy gap between HOMO and LUMO is very small and intermolecular interactions are sufficiently large [3].

Since planar π -conjugated molecules tend to stack to form the column structure, molecular metals developed in the early stage have the one-dimensional electronic structure which is characterized by a pair of planar Fermi surfaces and is associated with a metal-insulator transition at low temperatures. In order to achieve the stable metallic state down to low temperatures, much effort to increase the dimensionality of the electronic structure has been made by means of chemical modification and/or application of pressure. An organic donor BEDT-TTF (Fig. 1), where sulfur-containing six-membered rings attached to the TTF moiety effectively enhance the two-dimensional intermolecular interaction, opened a new molecular design for higher dimensional electronic structure and provided various types of metallic and superconducting cation radical salts [4]. In the (2,5-disubstituted DCNQI)-Cu

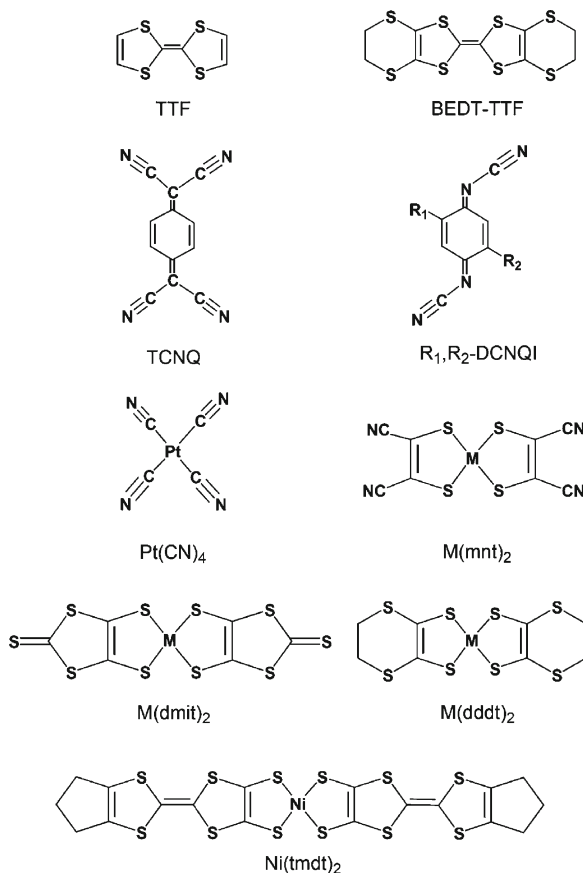


Fig. 1 Examples of component molecules for molecular conductors

salts, the $p\pi-d$ interaction between the acceptor molecule and the tetrahedrally coordinated Cu ion (in the mixed-valence state) forms a three-dimensional electronic structure [5].

Various mechanisms make the metallic state in the molecular system unstable. One is density wave (charge density wave and spin density wave) formation in the one-dimensional system, which can be removed by the increase of the dimensionality of the electronic structure. Even in the higher dimensional systems, however, the strong electron-electron correlation can induce the nonmetallic state. In systems with a half-filled energy band, where each unit in the crystal has one conduction electron, strong Coulomb interaction within the same site can induce an insulating state if the conduction band is narrow. This is a Mott insulating state. On the other hand, (typically) in systems with a quarter-filled band, strong Coulomb interaction between neighboring sites can induce inhomogeneous distribution of the site charges. This is a charge ordered insulating state.

The formal charge of $+1/2$ ($-1/2$) is the frequently observed valence state in the donor (acceptor) molecule in molecular conductors, which provides a quarter-filled hole (electron) band where the charge ordered state can occur. When the molecules are dimerized, the conduction band splits into bonding and antibonding pairs. If the degree of dimerization is strong, the upper and lower bands are largely separated by the dimerization gap and one of them is effectively half-filled. In this case, the system can behave like a half-filled system (one conduction electron on each dimer) and exhibit the Mott insulating state.

1.2 Molecular Conductors Based on Metal Complexes

In the early stage of the development of molecular conductors based on metal complexes, partially oxidized tetracyanoplatinate salts (for example, KCP; $K_2[Pt(CN)_4]Br_{0.30} \cdot 3H_2O$) and related materials were intensively studied [6]. In this system, the square-planar platinum complexes are stacked to form a linear Pt-atom chain. The conduction band originates from the overlap of $5dz^2$ orbitals of the central platinum atom and exhibits the one-dimensional character.

On the other hand, metal dithiolene complexes possess a delocalized electron system as a planar central core $M(C_2S_2)_2$. The conduction band is formed by the ligand π orbitals or mixed-metal-ligand orbitals where the sulfur atoms play an important role [7]. Depending on the choice of substituent groups attached to the central core, metal dithiolene complexes behave as both the donor and the acceptor. Development of molecular conductors based on the dithiolene complexes was triggered by the discovery of the metallic behavior in an anion radical salt $(H_3O)_{0.33}Li_{0.8}[Pt(mnt)_2] \cdot 1.67H_2O$ [8]. Among metal dithiolene complexes, the metal-dmit complexes $M(dmit)_2$ ($M = Ni$ and Pd ; Fig. 1) have been the most studied system. In the $M(dmit)_2$ molecule, HOMO has b_{1u} symmetry, while LUMO has b_{2g} symmetry. The metal d orbital can mix into the LUMO, but cannot contribute to the HOMO due to the symmetry, which destabilizes the HOMO and leads to a small energy splitting between HOMO and LUMO. The side-by-side intermolecular interaction, which leads to the formation of the two-dimensional electronic structure, is strong for the HOMO and weak for the LUMO. This is because some of overlap integrals for the intermolecular $S \cdots S$ pairs are canceled out due to the b_{2g} symmetry of the LUMO. Although the $M(dmit)_2$ molecule belongs to the acceptor, the nature of the conduction band in their anion radical salts strongly depends on the central metal. In general, the conduction band of the Pd system originates from the HOMO, while the conduction band of the Ni system originates from the LUMO. This unusual feature of the Pd system, HOMO-LUMO band inversion, is due to the strong dimerization and the small energy splitting between HOMO and LUMO [9]. In a series of anion radical salts with closed-shell cations (Cation) $[Pd(dmit)_2]_2$ (Cation = $Et_xMe_{4-x}Z^+$; $Z = N, P, As, Sb$ and $x = 0, 1, 2$), the dimer units $[Pd(dmit)_2]_2^-$ form a strongly correlated two-dimensional system with a quasi triangular lattice and exotic properties derived from frustration and strong

correlation are reported [7]. In these Pd salts, the choice of the counter cation tunes the degrees of frustration and correlation which are associated with the molecular arrangement. On the other hand, in the Ni salts, the choice of the counter cation provides a variety of molecular arrangements [7].

1.3 Molecular Conductors Based on Cationic Metal Complexes

Compared with the conducting anion radical salts of metal complexes, the number of molecular conductors based on cationic metal complexes is still limited. Donor type complexes $M(\text{dddt})_2$ ($M = \text{Ni}, \text{Pd}, \text{Pt}$; Fig. 1) are the most studied system. The $M(\text{dddt})_2$ molecule is a metal complex analogue of the organic donor BEDT-TTF. Formally, the central $\text{C}=\text{C}$ bond of BEDT-TTF is substituted by a metal ion. The HOMO and LUMO of the $M(\text{dddt})_2$ molecule are very similar in orbital character to those of the $M(\text{dmit})_2$ molecule. In addition, the HOMO of the $M(\text{dddt})_2$ molecule is also very similar to that of BEDT-TTF. More than ten cation radical salts of $M(\text{dddt})_2$ with a cation:(monovalent) anion ratio of 2:1 or 3:2 are reported [7]. A few of them exhibit metallic behavior down to low temperatures. The HOMO-LUMO band inversion can also occur in the donor system depending on the degree of dimerization. In contrast to the acceptor system, however, the HOMO-LUMO band inversion in the donor system leads a LUMO band with the one-dimensional character to the conduction band.

2 Unsymmetrical Components Based on Diimine–Dithiolene Complexes

2.1 Molecular Design of Unsymmetrical Components Based on Diimine–Dithiolene Complexes

Although there are a large number of symmetrical metal-dithiolene complexes as described in the previous section [7], only a few applications of mixed-ligand complexes have been reported as conducting materials [10]. Among various mixed-ligand complexes, a donor (HOMO)-metal-acceptor (LUMO) type molecule is capable of providing a new principle for the design of molecular conductors utilizing a potential interplay of intra- and intermolecular charge transfers (Fig. 2).

Pioneering work in this field was started in the 1980s by Matsubayashi et al. They suggested that planar $[(\text{N-N})\text{M}(\text{S-S})]^n$ ($M = \text{Ni}^{2+}, \text{Pd}^{2+}, \text{Pt}^{2+}, \text{Au}^{3+}$; $\text{N-N} = \text{phen}, \text{bpy}$ and $\text{Et-}, \text{Pr}^i\text{-}, \text{Bu-}, \text{Dec-}, \text{Hexdec-pia}$; $\text{S-S}^{2-} = \text{dmit}^{2-}$ and $\text{C}_8\text{H}_4\text{S}_8^{2-}$; $n = 0$ or $+1$) type unsymmetrical metal-dithiolene complexes would be good candidates for new components of molecular conductors [11–14]. The complexes, having HOMO on the dithiolene ligand and LUMO on the diimine ligand, are known to exhibit remarkable emission and luminescent spectra, due to their

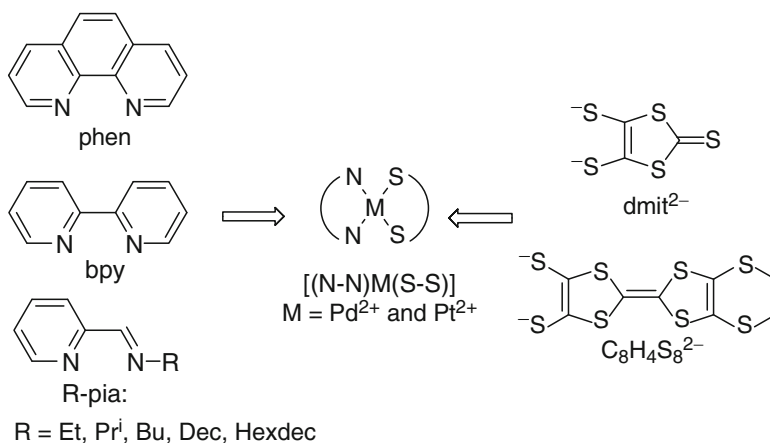


Fig. 2 Schematic drawing of unsymmetrical donors based on diimine-dithiolate complexes

unconventional electronic structures [15–21]. They have attempted to expand the field of conducting and magnetic materials by using the unsymmetrical molecules. For this purpose, a series of the diimine Pd^{2+} and Pt^{2+} complexes with the dithiolene ligands were prepared.

2.2 Cation Radical Salts of the Unsymmetrical Diimine–Dithiolene Complexes

2.2.1 Electrical Resistivities of the Cation Radical Salts

Matsubayashi et al. revealed donor abilities of the unsymmetrical diimine–dithiolene complexes [11–14]. The unsymmetrical complexes provided cation radical salts with various anions including I_3^- , Br_3^- and $TCNQ^-$ by use of chemical oxidation [11–14]. The electrical resistivities of the cation radical salts measured with their compressed pellets at room temperature are summarized in Table 1. The electrical resistivities of the dmit complexes were very high. The cation radical salts of the $C_8H_4S_8$ -complexes, which have the BEDT-TTF moiety [22, 23], exhibited lower resistivity than those of dmit complexes, except for $[(Bu-pia)Pt(C_8H_4S_8)]$ salts. However, crystal structures of these salts were not reported, and details of their electrical properties and electronic states were not discussed based on their crystal structures.

2.2.2 Crystal Structure of the Cation Radical Salt $[(bpy)Pt(C_8H_4S_8)][BF_4]$

Crystal structure data are indispensable for the discussion of the conduction mechanism in the cation radical salts based on the unsymmetrical complexes. In 2002,

Table 1 Cation radical salts based on the unsymmetrical donors and their electrical resistivities at room temperature

Complex	$\rho_{r.t.}, \Omega^{-1} \text{ cm}^{-1}$	Ref.
[(phen)Pt(dmit)]I _{2.2}	$>10^5$	[4]
[(bpy)Pt(dmit)]I _{1.9}	$>10^5$	[4]
[(Et-pia)Pt(dmit)]I _{1.9}	$>10^5$	[4]
[(Et-pia)Pt(dmit)]I _{3.4}	$>10^5$	[3]
[(Et-pia)Pt(dmit)]Br _{3.1}	$>10^5$	[3]
[(Pr ⁱ -pia)Pt(dmit)]I _{1.7}	$>10^5$	[4]
[(Dec-pia)Pt(dmit)]I _{3.3}	$>10^5$	[5]
[(Hexdec-pia)Pt(dmit)]I _{2.1}	$>10^5$	[5]
[(Bu-pia)Pd(dmit)]I _{1.8}	$>10^5$	[6]
[(bpy)Pt(C ₈ H ₄ S ₈)]I _{2.7}	7.7×10^2	[6]
[(bpy)Pt(C ₈ H ₄ S ₈)]TCNQ _{0.8}	1.5×10^2	[6]
[(Bu-pia)Pt(C ₈ H ₄ S ₈)]I ₃	$>10^5$	[6]
[(Bu-pia)Pt(C ₈ H ₄ S ₈)]TCNQ _{0.6}	$>10^5$	[6]
[(Bu-pia)Pd(C ₈ H ₄ S ₈)]I _{5.1}	7.1×10^2	[6]
[(Bu-pia)Pd(C ₈ H ₄ S ₈)]TCNQ _{0.4}	3.1×10^2	[6]

the first crystal structure analysis of a 1:1 cation radical salt based on the unsymmetrical diimine-dithiolene Pt complex [(bpy)Pt(C₈H₄S₈)] [BF₄] was reported by Kubo et al. [24]. Constant current electrolysis of a CH₂Cl₂ solution of [(bpy)Pt(C₈H₄S₈)] in the presence of (Bu₄N)(BF₄) afforded needles of a one-electron oxidized species [(bpy)Pt(C₈H₄S₈)] [BF₄] [14, 24, 25]. The crystal structure viewed along the *b* and *c* axes is shown in Fig. 3. The cation moieties are stacked with the same molecular orientation to form columnar structure along the *c* axis. S...S contacts shorter than van der Waals radii ($<3.7 \text{ \AA}$) are observed within and between the columns. The electrical resistivity of the salt measured with a compressed pellet at room temperature was $2.5 \times 10^2 \Omega \text{ cm}$. However, no data of temperature dependence of resistivity and electronic structure has been reported.

2.3 Conclusion

Matsubayashi et al. developed a new research field of molecular conductors by using the unsymmetrical diimine-dithiolene complexes. Various components with dmit and C₈H₄S₈ as dithiolene ligands were prepared. The unsymmetrical metal complexes provided various cation radical salts. Their electrical resistivities were measured with their compressed pellets at room temperature. The salt of the complexes with the C₈H₄S₈ ligand exhibited lower resistivity than that of the salt with the dmit ligand. No crystallographic data was reported. Thus, the details of the conducting mechanism of these salts cannot be discussed. The first crystal structure analysis was reported for the 1:1 salt [(bpy)Pt(C₈H₄S₈)] [BF₄].

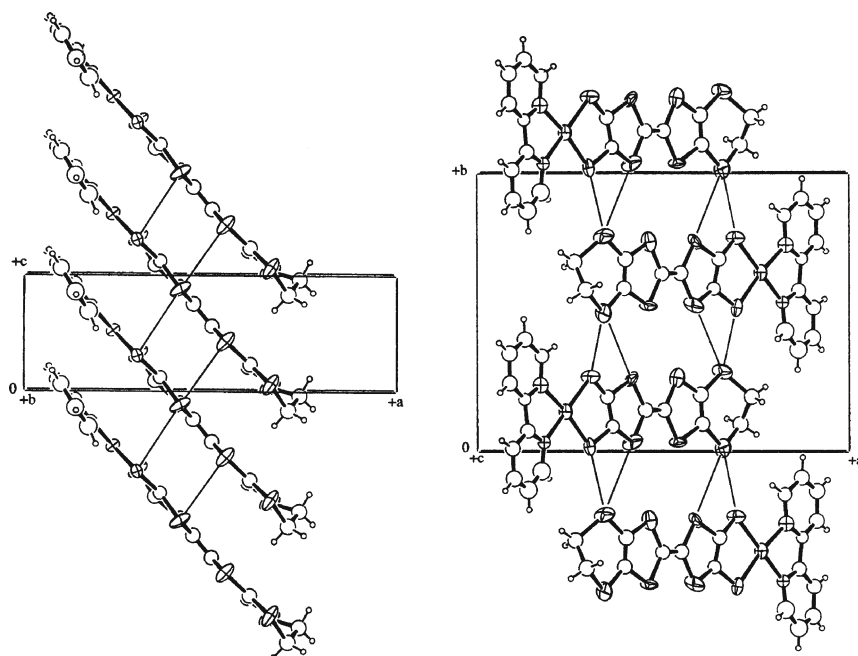
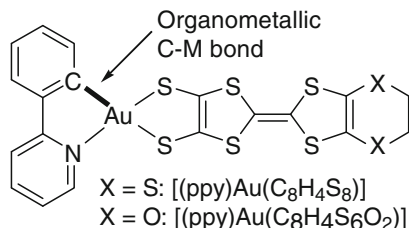


Fig. 3 Crystal structure depicted on the basis of the result described in [24]. (Reprinted with permission from [24]. Copyright 2002 Elsevier)

3 Unsymmetrical Components Based on Organometallic–Dithiolene Complexes

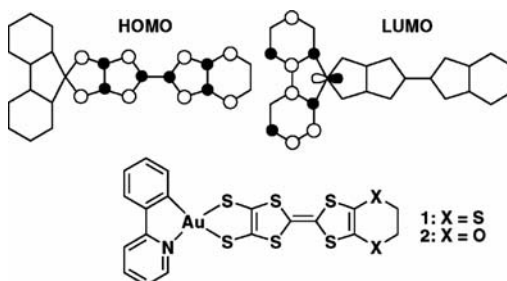
3.1 General Features of Unsymmetrical Components Based on Organometallic Metal–Dithiolene Complexes

The electronic state of this type of mixed-ligand unsymmetrical components can be modified by the combination of metal ions, nitrogen and sulfur-ligands. Kubo et al. modified the unsymmetrical complexes by an introduction of the carbon-metal σ -bond to improve the crystal quality and the conducting properties of their cation radical salts. They prepared the organometallic donor $[(ppy)Au(C_8H_4S_8$ or $C_8H_4S_8O_6)]$ (Scheme 1) and studied the electronic structures of the molecules [26, 27]. The organometallic gold complexes have the same molecular structure and charge with those of $[(bpy)Pt(C_8H_4S_8)]$ (see Sect. 2.1). However, orthometalated chelating ligands such as ppy^- can modify the electronic structure of diimine complexes, because of its asymmetry and the strong σ -bonding of the phenyl carbon atom [28–34]. The distributions of the HOMO and LUMO in these orthometalated compounds are analogous to those of the diimine complexes (Fig. 4) [36]. However, the lowest charge transfer excited states of the square-planar d_8 complex $[(ppy)Au$



Scheme 1 Schematic drawing of unsymmetrical organometallic donors

Fig. 4 HOMO and LUMO of the unsymmetrical organometallic gold-dithiolene complexes. (Reprinted with permission from [35]. Copyright 2008 American Chemical Society)



(C₈H₄S₈ or C₈H₄S₆O₂)] are not similar to that of [(bpy)Pt(C₈H₄S₈)] due to the orthometalation. In addition, the energy levels of the ground states for the orthometalated complexes are lower than those of the related diimine complexes [26, 27]. First redox potentials and HOMO-LUMO gaps of [(bpy)Pt(C₈H₄S₈)] and [(ppy)Au(C₈H₄S₈)] are summarized in Table 2. Donor ability of the organometallic gold complex is lower than that of the bpy-platinum complex. The HOMO-LUMO gap of the organometallic donor is larger than that of the bpy-platinum complex [14, 26]. Therefore, the σ -bond coordination markedly affects the HOMO and LUMO energy levels on the complexes. The organometallic Au complexes can form air stable crystal (Fig. 5), and provide various single crystals of their 2:1 cation radical salts by use of electrochemical crystallization [26, 27]. The 2:1 salts are more advantageous for improvement of their conducting properties than the 1:1 salts such as [(bpy)Pt(C₈H₄S₈)] [BF₄] (see Sect. 2.2.2) [22, 23].

3.2 Cation Radical Salts of the Organometallic Au(III) Dithiolene Complexes

Various cation radical salts [(ppy)Au(S-S)]₂[anion][solvent]_n (S-S = C₈H₄S₈ or C₈H₄S₆O₂, anion = PF₆⁻, BF₄⁻, AsF₆⁻, TaF₆⁻, solvent = PhCl, *n* = 0–0.5) were prepared by constant current electrolysis of their benzonitrile or chlorobenzene solutions containing (Bu₄N)(anion) as electrolyte [26, 27, 35, 37].

Table 2 First redox potentials and HOMO-LUMO gaps of [(bpy)Pt(C₈H₄S₈)] and [(ppy)Au(C₈H₄S₈)]

	[(bpy)Pt(C ₈ H ₄ S ₈)]	[(ppy)Au(C ₈ H ₄ S ₈)]
First redox potential (V vs Ag/Ag ⁺)	−0.2	+0.09
HOMO-LUMO gap (eV)	2.1	2.7

3.2.1 Crystal Structures

[(ppy)Au(C₈H₄S₈)]₄[anion]₂[PhCl]: anion = AsF₆[−], TaF₆[−]

The packing diagram of [(ppy)Au(C₈H₄S₈)]₄[AsF₆]₂[PhCl] is shown in Fig. 6. This crystal contains four crystallographically independent cation radicals, two octahedral anions and a solvent molecule in the asymmetric unit [27]. The cation radicals form tetramers with a head-to-head configuration, and the crystal structure consists of stacking of the tetramers along the *a*–*c* direction with alternate orientations. There are some S···S nonbonded contacts (3.61–3.68 Å) between the cation moieties (Fig. 6b). Solvent molecules, PhCl and counter ions, AsF₆[−] are situated between the cation columns (Fig. 6a). The crystal structure of the TaF₆ salt is similar to that of the AsF₆ salt [27].

[(ppy)Au(C₈H₄S₈)]₂[PF₆] and [(ppy)Au(C₈H₄S₈O₆)]₂[BF₄]

The cation radical salts [(ppy)Au(C₈H₄S₈)]₂[PF₆] (PF₆ salt) and [(ppy)Au(C₈H₄S₈O₆)]₂[BF₄] (BF₄ salt) exhibit different donor arrangements from those in the AsF₆ and TaF₆ salts. For each crystal, the asymmetric unit contains two cations and one anion. Columnar structures are formed by twofold head-to-head stacking of the cation radicals in the manner ···ABAB··· (Fig. 7a, b) [27, 35, 37]. Figure 7c, d shows side-views of the columns. Significant difference is observed in the distances between the molecular planes. This difference corresponds to the different overlapping modes in the PF₆ and BF₄ salts, as shown in Fig. 7e, f. The intermolecular interactions between oxygen and hydrogen atoms in the C₈H₄S₆O₂ moiety are observed along the stacking direction in the BF₄ salt (Fig. 7d) [38]. For the PF₆ salt, many intermolecular S···S contacts (3.339–3.616 Å) shorter than the van der Waals distance (<3.7 Å) are observed within the column, as well as between the columns (Fig. 7a). However, only the intercolumn S···S contacts are observed in the BF₄ salt (3.686 Å, Fig. 7b).

3.2.2 Electrical Properties of the Cation Radical Salts

[(ppy)Au(C₈H₄S₈)]₄[anion]₂[PhCl]: anion = AsF₆[−], TaF₆[−]

The AsF₆ and TaF₆ salts exhibit semiconducting behavior ($\rho_{\text{r.t.}} = 4.0 \times 10^2$ – 4.0×10^3 Ω cm; $E_{\text{a}} = 0.11$ – 0.15 eV) at ambient pressure. In the crystals, there are some

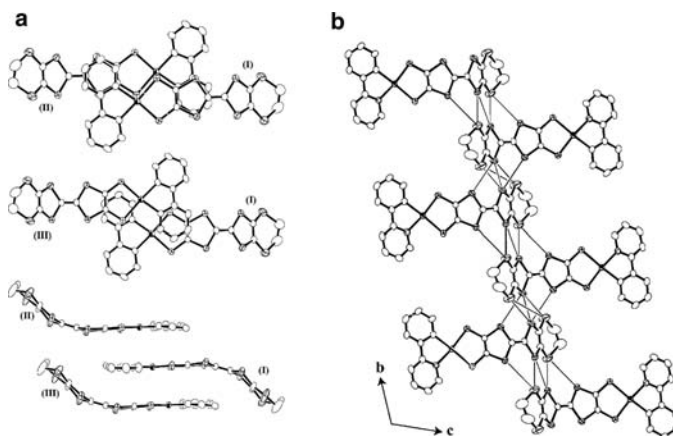


Fig. 5 (a) Molecular arrangements viewed along the molecular planes. (b) Packing diagram viewed along the bc plane in $[(\text{ppy})\text{Au}(\text{C}_8\text{H}_4\text{S}_8)]$. Fine lines show sulfur-sulfur contacts ($< 3.7 \text{ \AA}$) (Reprinted with permission from [26]. Copyright 2003 Elsevier)

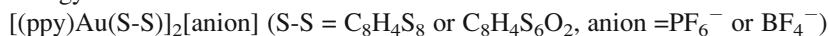
S...S contacts. However, conducting pathways are not formed effectively by the stacking of the cation radicals [26].



The PF_6 salt exhibits semiconductive behavior with a small activation energy ($\rho_{\text{r.t.}} = 2.6 \Omega \text{ cm}$; $E_a = 0.03 \text{ eV}$) at ambient pressure. The small activation energy suggests that the PF_6 salt is situated close to the metallic state (see Sect. 3.2.3.2). The application of pressure is an effective method to enhance the intermolecular interactions and the band width. Indeed, metallic behavior appears above 0.8 GPa. In addition, at 1.6 GPa, the metallic region reaches down to 20 K (Fig. 8). To our knowledge, the PF_6 salt is the first example of the metallic organometallic compound, even though pressure is required to achieve this state [35]. On the other hand, the BF_4 salt is highly insulating ($\rho_{\text{r.t.}} > 1 \times 10^5 \Omega \text{ cm}$) at ambient pressure and room temperature.

3.2.3 Electronic States of the Cation Radical Salts of Organometallic Metal–Dithiolene Complexes

Energy Band Structures of the Cation Radical Salts



Energy band calculation, spectroscopic and magnetic measurements are powerful methods to investigate the electronic states of the molecular conductors. Figure 9 shows energy band structures of the cation radical salts $[(\text{ppy})\text{Au}(\text{C}_8\text{H}_4\text{S}_8)]_2[\text{PF}_6]$ (PF_6 salt) and $[(\text{ppy})\text{Au}(\text{C}_8\text{H}_4\text{S}_8\text{O}_6)]_2[\text{BF}_4]$ (BF_4 salt) calculated by the tight-

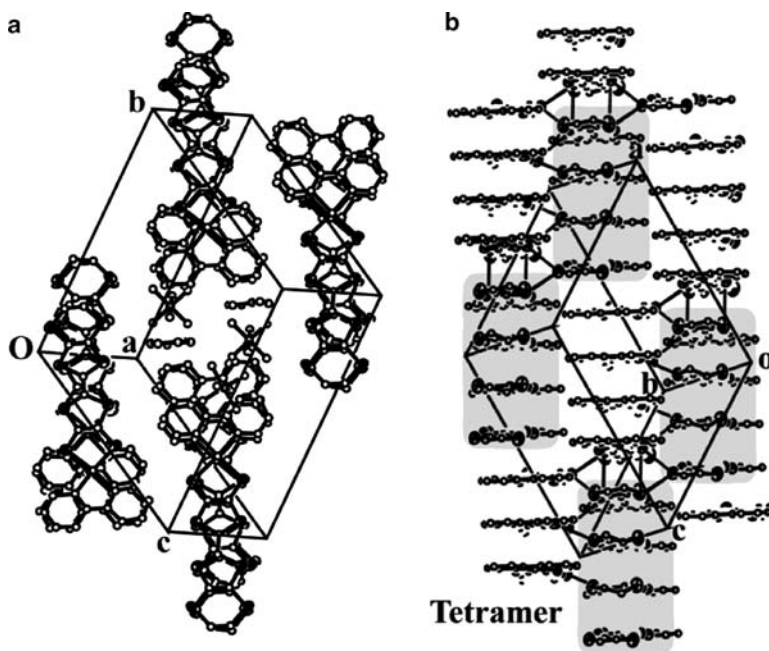


Fig. 6 (a) Crystal structure of $[(ppy)Au(C_8H_4S_8)]_4[AsF_6]_2[PhCl]$ along the molecular stacking direction. (b) End-on view of cation moieties of $[(ppy)Au(C_8H_4S_8)]_4[AsF_6]_2[PhCl]$. Fine lines indicate sulfur-sulfur contacts shorter than the van der Waals radii ($<3.7 \text{ \AA}$). (Reprinted with permission from [27]. Copyright 2005 Elsevier)

binding method with the extended Hückel MO calculation on the basis of the structural data [35]. The results of the calculations show that the difference in the cation arrangements provides remarkable distinctions of the electronic structure. The overlap integrals between HOMOs indicate strong dimerization in the BF_4 salt, while the cations are weakly dimerized in the PF_6 salt (Table 3). The band calculations suggest that the PF_6 salt has a one-dimensional metallic band structure with two pairs of planar Fermi surfaces. On the other hand, the BF_4 salt is a band insulator. This result is consistent with the resistivity measurements of the BF_4 salt. Thus, the BF_4 salt is a band insulator. However, the band calculation does not agree with the electrical resistivity measurement for the PF_6 salt which is due to the strong electron correlation in the salt as discussed in the next section [35].

Electronic State of $[(ppy)Au(C_8H_4S_8)]_2[PF_6]$

Temperature dependence of magnetic susceptibility of the PF_6 salt was measured from 300 to 4 K at 5 T [35]. The spin susceptibility of this salt gradually decreases from 300 to 50 K. Below 50 K, the susceptibility exhibits a rapid decrease accompanied by anisotropic temperature dependence, which is an indication of the long-range antiferromagnetic ordering. A one-dimensional Heisenberg model is

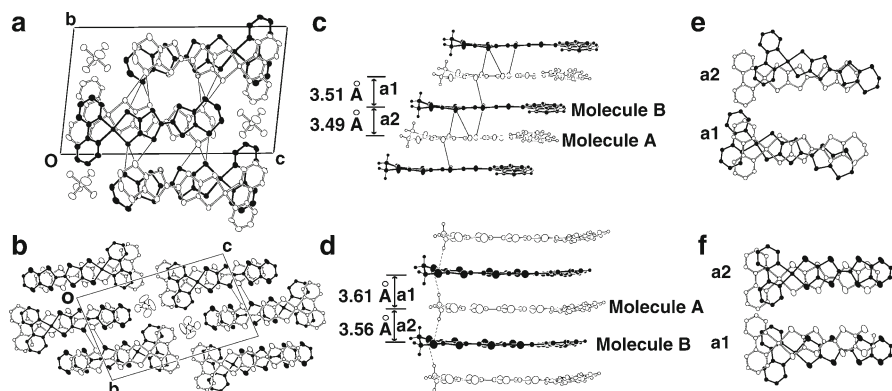


Fig. 7 Packing diagrams of (a) $[(\text{ppy})\text{Au}(\text{C}_8\text{H}_4\text{S}_8)]_2[\text{PF}_6]$ (PF_6 salt) and (b) $[(\text{ppy})\text{Au}(\text{C}_8\text{H}_4\text{S}_6\text{O}_2)]_2[\text{BF}_4]$ (BF_4 salt) viewed along the a axis. Side-views of the columns in the (c) PF_6 salt and (d) BF_4 salt. Molecular arrangements of two crystallographically independent molecules within the column of (e) PF_6 salt and (f) BF_4 salt. *Fine lines* indicate $\text{S}\cdots\text{S}$ contacts shorter than 3.7 Å. *Dashed lines* indicate $\text{O}\cdots\text{H}$ contacts within the range of 2.62–2.70 Å. (Reprinted with permission from [35]. Copyright 2008 American Chemical Society)

applicable to the data above 100 K. The reflectance spectrum indicates an evidently dimeric structure. From the Raman and IR measurements, no charge ordering was found [35]. All these results indicate that the PF_6 salt is an effectively half-filled system due to the (weak) dimerization and a paramagnetic insulator with a localized $S = 1/2$ spin on each dimer at ambient pressure (Fig. 10). That is, this system is a quasi-one-dimensional Mott insulator based on the dimer unit of uniformly charged donor molecules with a site-charge of +0.5. This means that the band crossing of the second and third subbands (ii) and (iii) in Fig. 9a is an artifact of the calculation and the actual band structure has a gap between subbands (ii) and (iii). However, this artifact suggests that the dimerization gap is expected to be narrow and the antiferromagnetic Mott insulating state is situated in the vicinity of the metal-insulator boundary [35]. One possible mechanism of the pressure-induced metallic state is a removal of the effective half-filled state. If the subbands (ii) and (iii) hybridize well with each other under pressure, the effectively half-filled state turns to the quarter-filled state with wider band width.

3.3 Conclusion

New molecular architecture of the components for molecular conductors was developed by using the unsymmetrical organometallic-dithiolene complexes which were modified from the unsymmetrical diimine-dithiolene complexes by the introduction of carbon-metal σ -bond. Two organometallic donor components with $\text{C}_8\text{H}_4\text{S}_8$ and $\text{C}_8\text{H}_4\text{S}_6\text{O}_2$ as the dithiolene ligands were synthesized and their 2:1 cation radical salts $[(\text{ppy})\text{Au}(\text{S-S})]_2[\text{anion}][\text{solvent}]_n$ ($\text{S-S} = \text{C}_8\text{H}_4\text{S}_8$ or $\text{C}_8\text{H}_4\text{S}_6\text{O}_2$, anion = PF_6^- , BF_4^- , AsF_6^- , TaF_6^- , solvent = PhCl , $n = 0\text{--}0.5$) were prepared as

Fig. 8 Temperature dependence of the resistivity for $[(\text{ppy})\text{Au}(\text{C}_8\text{H}_4\text{S}_8)]_2[\text{PF}_6]$ at various pressures from ambient pressure to 1.6 GPa. (Reprinted with permission from [35]. Copyright 2008 American Chemical Society)

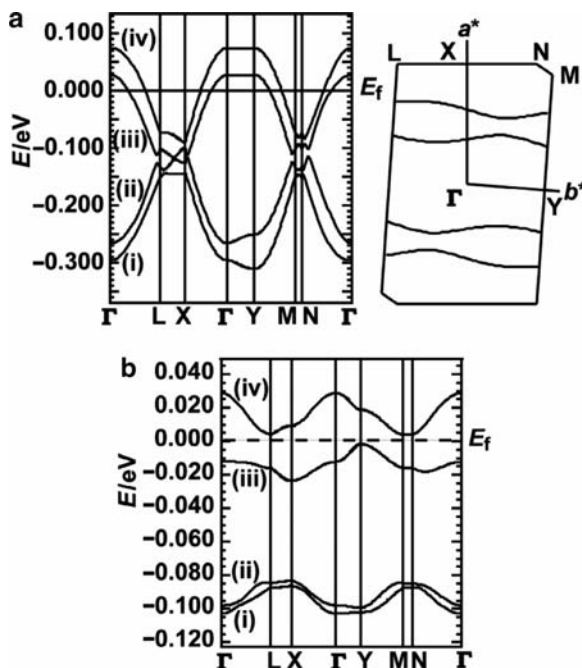
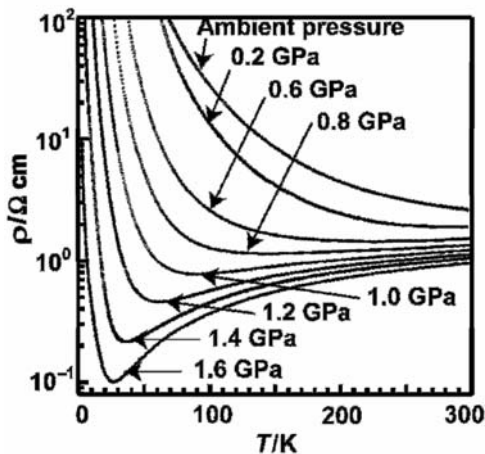


Fig. 9 Energy band structures of: (a) $[(\text{ppy})\text{Au}(\text{C}_8\text{H}_4\text{S}_8)]_2[\text{PF}_6]$; (b) $[(\text{ppy})\text{Au}(\text{C}_8\text{H}_4\text{S}_8\text{O}_6)]_2[\text{BF}_4]$. (Reprinted with permission from [35]. Copyright 2008 American Chemical Society)

single crystals by electrochemical crystallization. $[(\text{ppy})\text{Au}(\text{C}_8\text{H}_4\text{S}_8)]_2[\text{PF}_6]$ under pressure is the first molecular metal based on the organometallic component. At ambient pressure, this system is the Mott insulator in the vicinity of the metal-insulator boundary. Other salts are band insulators.

Table 3 Calculated overlap integrals (S) between HOMOs for the cation radical salts the PF_6 and BF_4 salts. (Reprinted with permission from [35]. Copyright 2008 American Chemical Society)

$S (\times 10^{-3})$	PF_6 salt	BF_4 salts
a1	−8.3	−0.8
a2	−9.0	−4.6
b1	1.3	−0.2
b2	−1.9	−0.4
b3	1.1	−1.5
b4	−1.2	−0.2
p1	−1.2	−0.7
p2	−0.9	−0.2

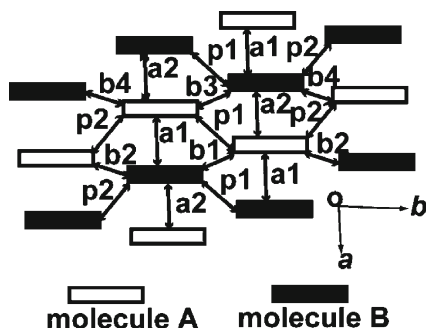
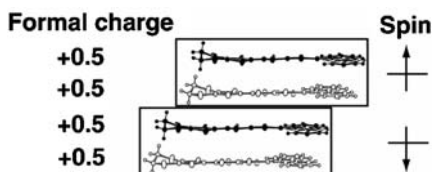


Fig. 10 Schematic display of the electronic structure of $[(\text{ppy})\text{Au}(\text{C}_8\text{H}_4\text{S}_8)_2][\text{PF}_6]$ at ambient pressure (Reprinted with permission from [35]. Copyright 2008 American Chemical Society)



4 Other Unsymmetrical Organometallic–Dithiolene Complexes for the Components of Molecular Conductors

The molecular charge of the organometallic complexes shown in Scheme 1 can be modified easily by the choice of the metal ions. Suga et al. prepared monovalent organometallic platinum–dithiolene complexes which have the same molecular structure with that of the gold complexes (Figs. 11 and 12), and succeeded in obtaining neutral radicals of the organometallic platinum–dithiolene complex by chemical oxidation [39]. These neutral radicals can be expected to develop toward new type of single component molecular conductors [3], although these neutral radicals are insulators and their crystal structures have not been revealed yet.

5 General Conclusion

Chemical research of molecular metals was activated by the discovery of the metallic charge transfer salt TTF–TCNQ in 1973 [40]. Two basic molecular architectures have been studied intensively. One is based on organic molecules with the

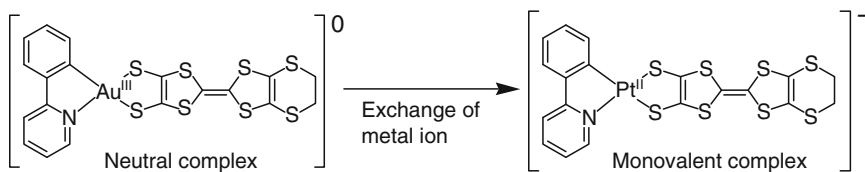


Fig. 11 Schematic drawing of neutral and monovalent complexes based on the organometallic-dithiolene compounds

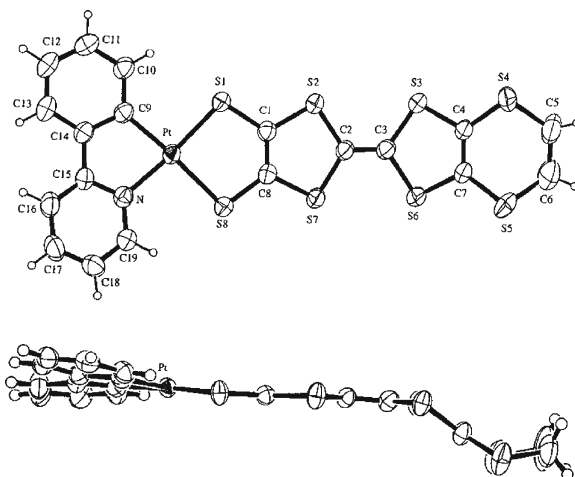


Fig. 12 Anion moiety in $(\text{Bu}_4\text{N})[(\text{ppy})\text{Pt}(\text{C}_8\text{H}_4\text{S}_8)]$. (Reprinted with permission from [39]. Copyright 2004 Chemical Society of Japan)

TTF moiety such as BEDT-TTF. The other is based on metal-dithiolene complexes such as $M(\text{dmit})_2$. Both architectures succeeded in providing various highly conducting materials which exhibit superconducting and metallic behavior. Researches of the molecular conductors have focused on the fundamental aspects of the science of molecular conductors. Recently, however, the molecular conductors have been applied to functional materials such as nano devices. New molecular architectures for control of crystal structures and electronic properties have been required. Matsubayashi et al. proposed new molecular architecture by using the unsymmetrical diimine-dithiolene complexes. They have established the basic chemistry of the complexes by spectroscopic and electrochemical measurements and revealed conducting properties of the salt containing the unsymmetrical complexes, although the single crystals were not obtained. Modification of the unsymmetrical molecules by the introduction of the carbon-metal σ -bond was examined in order to improve crystal quality and the conducting ability of their cation radical salts. Kubo et al. have succeeded in preparation of the first organometallic components by the modification of the unsymmetrical complexes and their 2:1 cation radical salts as

single crystals. Among them, the cation radical salt [(ppy)Au(C₈H₄S₈)₂][PF₆] is the first metallic compound derived from organometallic compounds, even though pressure is required to achieve the metallic state. This has opened the way to the basic science of the electrically conducting organometallic compounds. This type of organometallic complex can easily change their molecular charge by the choice of the ligands and metal ions. Suga et al. have succeeded in preparation of neutral radicals based on the unsymmetrical platinum dithiolene complexes for new type of single components molecular conductors. Although the number of reports on molecular conductors derived from the organometallic complexes is limited at present, the organometallic compounds would be the vast frontiers of molecular conductors.

References

1. Akamatu H, Inokuchi H, Matsunaga Y (1954) *Nature* 173:168
2. Mori T, Kobayashi A, Sasaki Y, Kobayashi H, Saito G, Inokuchi H (1984) *Bull Chem Soc Jpn* 57:627
3. Tanaka H, Okano Y, Kobayashi H, Suzuki W, Kobayashi A (2001) *Science* 291:285
4. Kagoshima S, Kato R, Fukuyama H, Seo H, Kino H (1999) In: Bernier P, Lefrant S, Bidan G (eds) *Advances in synthetic metals – twenty years of progress in science and technology*. Elsevier Science, Amsterdam, p 262
5. Kato R (2000) *Bull Chem Soc Jpn* 73:515
6. Miller JS, Epstein AJ (1976) *Prog Inorg Chem* 20:1
7. Kato R (2004) *Chem Rev* 104:5319 and references cited therein
8. Underhill AE, Ahmad MM (1981) *J Chem Soc Chem Commun* 67
9. Canadell E, Ravy S, Pouget JP, Brossard L (1990) *Solid State Commun* 75:633
10. Watanabe E, Fujiwara M, Yamaura JI, Kato R (2001) *J Mater Chem* 11:2131
11. Matsubayashi G, Yamaguchi Y, Tanaka T (1988) *J Chem Soc Dalton Trans* 2215
12. Matsubayashi G, Hirao M, Tanaka T (1988) *Inorg Chim Acta* 144:217
13. Nakahama A, Nakano M, Matsubayashi G (1999) *Inorg Chim Acta* 284:55
14. Kubo K, Nakano M, Tamura H, Matsubayashi G (2000) *Inorg Chim Acta* 311:6
15. Miller TR, Dance IG (1973) *J Am Chem Soc* 95:6970
16. Vogler A, Kunkely H, Hlavatsch J, Merz A (1984) *Inorg Chem* 23:506
17. Zuleta JA, Bevilacqua JM, Proserpio DM, Harvey PD, Eisenberg R (1992) *Inorg Chem* 31:2396
18. Paw W, Cummings SD, Mansour MA, Connick WB, Geiger DK, Eisenberg R (1998) *Coord Chem Rev* 171:125
19. Cocker TM, Bachman RE (2001) *Inorg Chem* 40:1550
20. Makedonas C, Mitsopoulou CA, Lahoz FJ, Balana AI (2003) *Inorg Chem* 42:8853
21. Chen CT, Liao SY, Lin KJ, Chen CH, Lin TYJ (1999) *Inorg Chem* 38:2734
22. Shibaeva RP, Yagubskii EB (2004) *Chem Rev* 104:5347 and references cited therein
23. Kobayashi H, Cui HB, Kobayashi A (2004) *Chem Rev* 104:5265 and references cited therein
24. Kubo K, Nakano M, Tamura H, Matsubayashi G (2002) *Inorg Chim Acta* 336:120
25. Matsubayashi G, Nakano M, Tamura H (2002) *Coord Chem Rev* 226:143
26. Kubo K, Nakano M, Tamura H, Matsubayashi G, Nakamoto M (2003) *J Organomet Chem* 669:141
27. Kubo K, Nakao A, Ishii Y, Kato R, Matsubayashi G (2005) *Synth Met* 153:425
28. Mdleleni MM, Bridgewater JS, Watts RJ, Ford PC (1995) *Inorg Chem* 34:2334

29. Schmid B, Garces FO, Watts RJ (1994) *Inorg Chem* 33:9
30. Craig CA, Watts RJ (1989) *Inorg Chem* 28:309
31. Ichimura K, Kobayashi T, King KA, Watts RJ (1987) *J Phys Chem* 91:6104
32. Ohsawa Y, Sprouse S, King KA, DeArmond MK, Hanck KW, Watts RJ (1987) *J Phys Chem* 91:1047
33. Sprouse S, King KA, Spellane PJ, Watts RJ (1984) *J Am Chem Soc* 106:6647
34. King KA, Spellane PJ, Watts RJ (1985) *J Am Chem Soc* 107:1431
35. Kubo K, Nakao A, Ishii Y, Yamamoto T, Tamura M, Kato R, Yakushi K, Matsubayashi M (2008) *Inorg Chem* 47:5495
36. Mansour MA, Lachicotte RJ, Gysling HJ, Eisenberg R (1998) *Inorg Chem* 37:4625
37. Kubo K, Nakano M, Tamura H, Matsubayashi G (2003) *Eur J Inorg Chem* 4093
38. Horiuchi S, Yamochi H, Saito G, Sakaguchi KI, Kusunoki M (1996) *J Am Chem Soc* 118:8604
39. Suga Y, Nakano M, Tamura H, Matsubayashi G (2004) *Bull Chem Soc Jpn* 77:1877
40. Ferraris J, Cowan DO, Walatka V, Perlstein JH (1973) *J Am Chem Soc* 95:948

Conducting and Magnetic Organometallic Molecular
Materials

Fourmigué, M.; Ouahab, L. (Eds.)

2009, XII, 193 p. 104 illus., 22 illus. in color., Hardcover

ISBN: 978-3-642-00407-0